EPIDEMIOLOGY

Social network plasticity decreases disease transmission in a eusocial insect

Nathalie Stroeymeyt[1]*†, Anna V. Grasse[2], Alessandro Crespi[3], Danielle P. Mersch[1]‡, Sylvia Cremer[2]†, Laurent Keller[1]†

Animal social networks are shaped by multiple selection pressures, including the need to ensure efficient communication and functioning while simultaneously limiting disease transmission. Social animals could potentially further reduce epidemic risk by altering their social networks in the presence of pathogens, yet there is currently no evidence for such pathogen-triggered responses. We tested this hypothesis experimentally in the ant *Lasius niger* using a combination of automated tracking, controlled pathogen exposure, transmission quantification, and temporally explicit simulations. Pathogen exposure induced behavioral changes in both exposed ants and their nestmates, which helped contain the disease by reinforcing key transmission-inhibitory properties of the colony's contact network. This suggests that social network plasticity in response to pathogens is an effective strategy for mitigating the effects of disease in social groups.

Social insects are an ideal system to study the potential role of social network plasticity in disease defense. The networks of social and physical interactions of insect, vertebrate, and human societies share many properties that are known to influence disease spread (*1*–*11*). In addition, because the high genetic similarity and frequent physical contacts between individuals heighten the risk of infection transmission within colonies, social insects have evolved a variety of collective mechanisms to prevent infection and limit the spread of pathogens through the colony [social immunity, (*12*, *13*)]. In particular, the organization of the colony into distinct age-and-task groups has been predicted to confer a double disease-related benefit by inhibiting global transmission dynamics and by disproportionately protecting high-value individuals (i.e., the queen and young workers) from pathogen exposure (*12*–*16*). We first tested these predictions in the absence of disease (constitutive organizational immunity) by using an automated ant tracking system to detect all physical contacts in 22 *Lasius niger* colonies and quantify transmission-relevant properties of their social networks (Fig. 1, A and B, and fig. S1). We focused on global network properties known to either inhibit or facilitate disease spread (see Table 1) and compared them to those of null model networks, obtained by randomizing the identity of interacting ants while preserving the temporal properties of the contact sequence and the total number of contacts for each ant. The observed networks displayed transmission-inhibiting rather than transmission-enhancing properties: They had higher modularity, lower density, larger diameter, and lower mean and maximum degree centrality than the random networks (fig. S2 and table S1). To further test whether the ant network's overall topology does inhibit disease transmission, we developed a stochastic epidemiological model simulating the spread of a pathogen through the colony and parameterized it using experimental data on the transmission of conidiospores (hereafter "spores") of the fungus *Metarhizium brunneum*, a natural pathogen of *L. niger* ants (*12*, *17*, *18*). Our simulation model had high predictive power and outperformed simpler models in predicting the intensity and biological consequences of transmission across individuals (Fig. 2A and table S2). Simulations confirmed that, relative to the random networks, the topology of the observed networks results in slower pathogen transmission, smaller amounts of pathogen transferred to nestmates, and a more-pronounced right skew in the distribution of final pathogen loads, which corresponds to a greater proportion of host individuals receiving a low, presumably harmless load (*19*) and a lower proportion of individuals receiving a high, potentially disease-inducing load (fig. S3 and table S1).

In addition to the overall network topology, the relative positions of individuals in the network also contributed to decrease disease impact. In social insects, new infections are more likely to be picked up by foragers outside the nest than by indoor workers (hereafter referred to as "nurses") (*12*, *13*), because the nest is subject to effective preventative hygienic treatments (*20*). Importantly, there was a strong negative relationship between degree centrality and time spent outside in the observed networks [general linear mixed model (GLMM) with type III Wald chi-square test: $\chi^2 = 402.9$, df = 1, $P < 0.0001$; fig. S4 and table S3], indicating that the ants that have a higher chance of encountering pathogens (i.e., frequent foragers) also have fewer connections within the network. This should confer important disease-related benefits because epidemic risk is reduced when the disease originates from nodes with few connections (*4*, *10*). In agreement with this prediction, simulations indicate that pathogens spread significantly more slowly and less broadly when they originate from frequent foragers than when they originate from occasional foragers, nurses, or random workers (fig. S5), showing that the ant social network provides strong colony-wide protection against the most likely source of disease. Moreover, analysis of the social organization of the 22 colonies in our main experiment and an additional 11 age-marked colonies ("age experiment") showed that *L. niger* colonies display marked segregation between potential disease sources (foragers) on one hand and high-value individuals (young workers acting as nurses and the queen) on the other (fig. S6). Simulations indicated that this organization disproportionately protects high-value individuals from the most likely source of disease (i.e., pathogens carried back to the nest by frequent foragers; fig. S7).

After describing the constitutive transmission-inhibitory characteristics of the ant social network, we tested whether colonies change their patterns of social contacts in an adaptive way when confronted with disease [induced organizational immunity (*14*, *21*)]. To do so, we randomly selected 10% of the colony's workers among foragers and exposed them either to a control solution (sham-treated colonies; $n = 11$) or to a suspension of *M. brunneum* spores (pathogen-exposed colonies; $n = 11$) and then returned them to the foraging arena. After a recovery period of 2 hours, the colony's behavior was tracked for an additional 24 hours, at which time we determined the spore load of each individual from pathogen-exposed colonies using quantitative, real-time PCR (qPCR; fig. S8). *M. brunneum* spores are transferred by physical contacts between ants, which can lead to the transmission of disease to healthy nestmates regardless of the future fate of the originally exposed ants (*19*). The spores typically penetrate the host's body to cause infection from 1 to 2 days after initial exposure (*22*), that is, after the end of the experiment. As a consequence, any behavioral changes induced by pathogen exposure should reflect an active response by the host rather than a manipulation by the pathogen or a side effect of disease because no infection could take place during the experiment. Additionally, because the pathogen did not start replicating during the experiment, the measured spore loads should closely reflect the contamination level of each ant depending on its position within the colony's contact

[1]Department of Ecology and Evolution, University of Lausanne, CH-1015 Lausanne, Switzerland. [2]Institute of Science and Technology Austria (IST Austria), Am Campus 1, A-3400 Klosterneuburg, Austria. [3]Biorobotics Laboratory, Ecole Polytechnique Fédérale de Lausanne, CH-1015 Lausanne, Switzerland.
*Present address: Laboratory of Intelligent Systems, Ecole Polytechnique Fédérale de Lausanne, CH-1015 Lausanne, Switzerland.
†Corresponding author. Email: laurent.keller@unil.ch (L.K.); nathalie.stroeymeyt@normalesup.org (N.S.); sylvia.cremer@ist.ac.at (S.C.) ‡Present address: Department of Physics of Complex Systems, Weizmann Institute of Science, Rehovot, Israel.

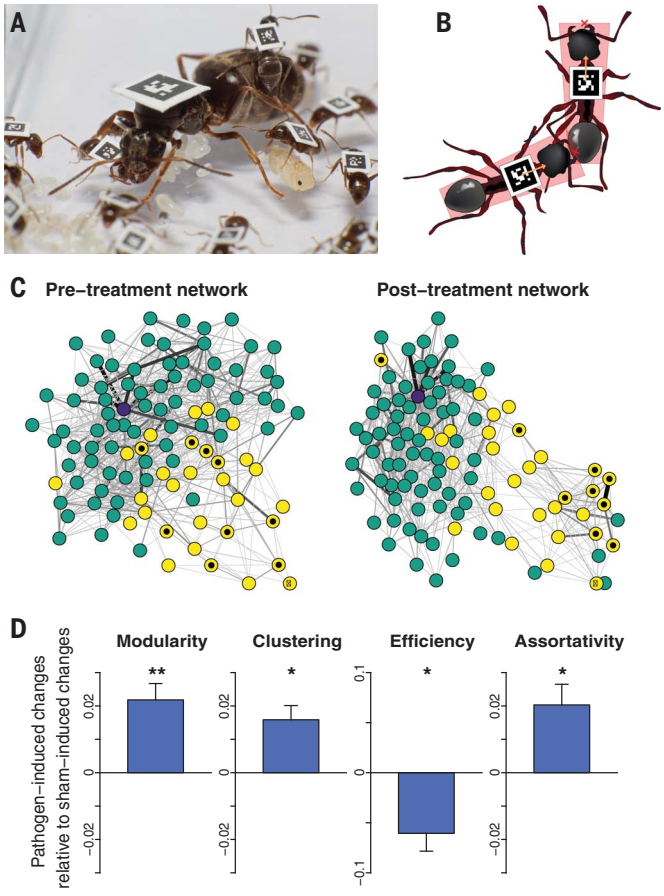

Fig. 1. Pathogen-induced changes in social networks. (**A**) Individually tagged *L. niger* queen (1.6-mm tag) and workers (0.7-mm tags). [Photo credit: T. Brütsch, University of Lausanne] (**B**) Geometrical approach used to infer physical contacts. Each ant is overlaid with a trapezoid (red), and a contact is recorded if the front end of the trapezoid of one ant overlaps with the trapezoid of the other ant. Red X's indicate the front end of the ants' trapezoids; orange arrows indicate the orientation of the ants' bodies. (**C**) Pre- and posttreatment networks from a pathogen-exposed colony. Each node represents an ant (queen, purple; nurses, green; foragers, yellow). Weighted edges represent the cumulated duration of contact between each pair of ants. Experimentally treated foragers are indicated with a black dot. (**D**) Pathogen-induced changes in network properties. For visualization of the results, bars and whiskers show the means and standard errors of the difference between post- and pretreatment values in pathogen-exposed colonies after subtraction of the mean difference in sham-treated colonies. Statistical analyses were performed on all raw data. *$P < 0.05$; **$P < 0.01$ (GLMM, interaction$_{period \times treatment}$). Sample sizes: 11 pathogen-exposed and 11 sham-treated colonies.

Table 1. Global network properties influencing disease transmission. Whenever relevant, network properties were calculated using weighted network edges. + indicates enhancement; − indicates inhibition.

Property	Definition	Effect on transmission
Modularity (*8*–*11*)	Degree of compartmentalization of the network into distinct communities of well-connected nodes	−
Clustering (*10*, *11*)	Tendency of neighboring nodes to form fully connected sets	−
Density (*1*)	Proportion of existing edges among all possible edges	+
Diameter (*6*)	Maximum length of the shortest paths between all pairs of nodes	−
Network efficiency (*28*)	Mean connection efficiency (i.e., inverse of the shortest path length) across all pairs of nodes	+
Degree centrality (*4*, *10*)	Number of edges connecting a node to other network nodes	+
Assortativity	Degree of preferential association between nodes of similar properties	Node-specific

network. Accordingly, we found a positive association between qPCR-measured pathogen transmission and network density, efficiency, and mean degree centrality on one hand and a negative association between measured pathogen transmission and network diameter, modularity, and clustering on the other (fig. S9), in agreement with theoretical predictions (table S1). Furthermore, qPCR results showed that untreated foragers received significantly higher amounts of spores from the experimentally treated foragers than either nurses or the queen [GLMM, $|z\ score| \geq 4.56$, $P < 0.0001$ in post hoc comparisons with Benjamini-Hochberg (BH) correction; Fig. 2B and table S3] and that the pathogen load received was significantly negatively correlated with network distance to treated ants (fig. S10). An additional experiment in which we exposed another 11 colonies to *M. brunneum* and allowed the disease to develop for 9 days ("survival experiment") further showed that pathogen-induced mortality was higher among untreated foragers than among nurses and that all queens were still alive at the end of the experiment (fig. S11). These results altogether confirm that the queen and nurses are effectively protected from disease carried back to the nest by foragers.

Comparisons of the network's structure before and after treatment revealed that pathogen exposure induced changes that should both reduce overall disease spread and reinforce the protection of high-value individuals. Indeed, relative to the sham treatment, pathogen exposure induced a strengthening of three of the network's transmission-inhibiting properties (increased modularity and clustering and decreased transmission efficiency), an increase in social segregation between task groups (increased task assortativity and increased network distances between the queen and workers), and a decrease in the spreading influence (degree centrality) of pathogen-exposed foragers [GLMM, global network properties, interaction between period and treatment (interaction$_{period \times treatment}$, where period is pre- versus posttreatment and treatment is sham versus pathogen-exposed): $\chi^2 \geq 4.25$, df = 1, $P \leq 0.039$ in all tests; individual node properties, post hoc comparisons with BH correction: $|z\ score| \geq 5.10$, $P < 0.0001$; Fig. 1, C and D, fig. S12, and table S3]. Simulations confirmed that these pathogen-induced changes in the social network protected the colony against disease by significantly reducing the probability of contamination and the number of spores received by untreated ants (GLMM, treatment-induced changes in sham-treated versus pathogen-exposed colonies: $\chi^2 \geq 6.26$, df = 1, $P \leq 0.012$; fig. S13 and table S3), which is consistent with our empirical findings (fig. S9). Simulations also confirmed that pathogen-induced network changes reinforced the protection of high-value individuals by significantly decreasing the probability of the queen and nurses receiving a high load, while simultaneously increasing their probability of receiving a low load (GLMM, queens: $\chi^2 \geq 5.08$, $P < 0.024$;

nurses: |z score| ≥ 8.38, $P < 0.0001$; foragers: |z score| ≤ 0.58, $P \geq 0.56$ in post hoc comparisons with BH correction; Fig. 3, A and B, and table S3). These findings are important because the consequences of contamination with *M. brunneum* have been shown to be highly dose-dependent in ants and termites: Whereas high-level contamination can lead to disease-induced death, low-level contamination is beneficial because it does not induce mortality and allows individuals to develop active immunization that protects them against future challenges with the same pathogen (*19*, *23*, *24*). Interestingly, converting the threshold used to distinguish high from low simulated dose (Fig. 3A) to a real exposure dose (Fig. 2A) revealed that it is in the same order of magnitude as a dose causing 2% mortality (lethal dose 2%, LD2) (table S4), which was identified as a dose inducing immunization in a related species (*19*). Thus, pathogen-induced network changes should confer a dual advantage for the colony because they simultaneously decrease the probability that the queen and nurses receive a potentially mortal load and increase the probability that they receive a harmless load leading to beneficial immunization. To test whether the high versus low

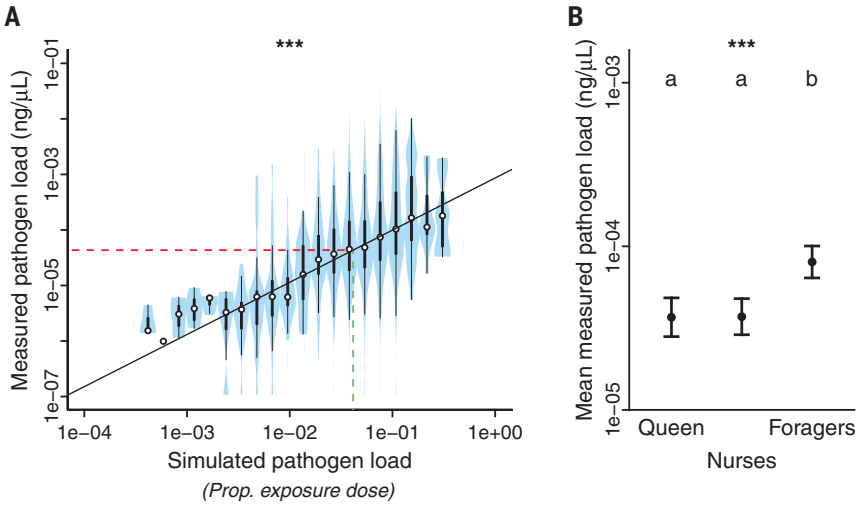

Fig. 2. Experimentally measured and simulated *M. brunneum* transmission in pathogen-exposed colonies. (**A**) Relationship between qPCR-measured pathogen loads and simulated pathogen loads (i.e., the total amount of pathogen received by each ant, averaged across 500 simulations of disease transmission and expressed as a proportion of the original load of treated foragers) in untreated ants. Simulations were run over the posttreatment networks using experimentally treated foragers as disease origin. Points represent the medians, thick black lines represent the interquartile ranges, thin black lines represent 1.5× the interquartile range, and violin shadings represent the density of individual data points. ***$P < 0.0001$ (GLMM). The dashed green line represents the threshold value identified from simulation results in Fig. 3A, and the dashed red line its corresponding value of measured pathogen load calculated using the fitted GLMM model. (**B**) Mean measured pathogen loads in untreated ants. Points represent the means, and whiskers represent the standard errors. ***$P < 0.0001$ (GLMM). Same letters (a and a) indicate $P = 0.96$ and different letters (a and b) indicate $P < 0.0001$ in post hoc comparisons (BH corrected). Sample size: 11 colonies from the main experiment and 11 colonies from the age experiment.

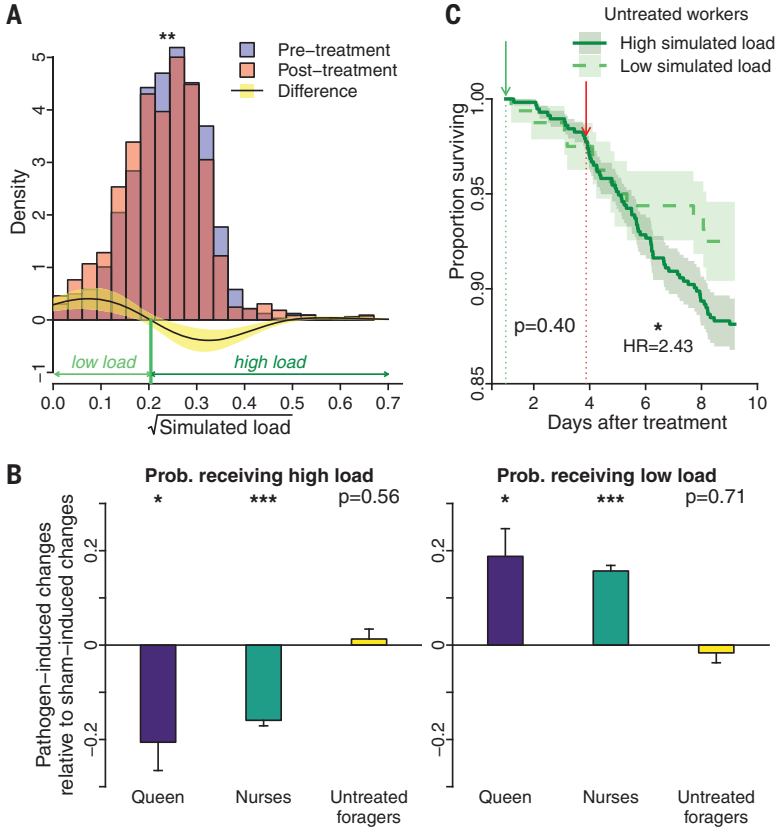

Fig. 3. Pathogen-induced changes in simulated disease transmission. (**A**) Density distributions of the simulated pathogen loads of untreated ants in simulations run over pretreatment and posttreatment networks (purple and peach histograms; overlap in mauve) in pathogen-exposed colonies. The black line and yellow shading represent the mean and standard error of the difference between post- and pretreatment distributions. The green line highlights the value at which there is an inversion in the sign of the density difference. This value was used as a threshold to distinguish high from low simulated loads in all subsequent analyses (e.g., in Fig. 3, B and C). Kolmogorov-Smirnov test, D statistic = 0.073, **$P = 0.006$. (**B**) Pathogen-induced changes in the probability of individuals receiving a high load or a nonzero low load in simulations. Visual representation as in Fig. 1F; statistical analysis on all raw data *$P < 0.05$; ***$P <$ 0.0001 (GLMM; post hoc comparisons between pathogen-induced and sham-induced changes, BH corrected). Sample sizes, pathogen-exposed/sham-treated colonies: 11/11 queens, 862/685 nurses, 214/284 untreated foragers and 105/94 treated workers. (**C**) Survival (lines) ± 95% confidence intervals (shaded areas) of untreated workers predicted to receive either a high load (dark green, solid line) or a low load (light green, dashed line) on the basis of simulations run over the first 24 hours posttreatment in the survival experiment. The green arrow represents the time of load prediction (1 day after treatment), and the red arrow represents the time at which an increase in mortality was detected among untreated ants (around 4 days after treatment; fig. S11). Mixed-effects Cox proportional hazard model comparing high- versus low-load workers, first 4 days: hazard ratio (HR) = 0.57, $\chi^2 = 0.71$, df = 1, $P = 0.40$; after day 4: HR = 2.43, $\chi^2 = 6.43$, df = 1, *$P = 0.011$.

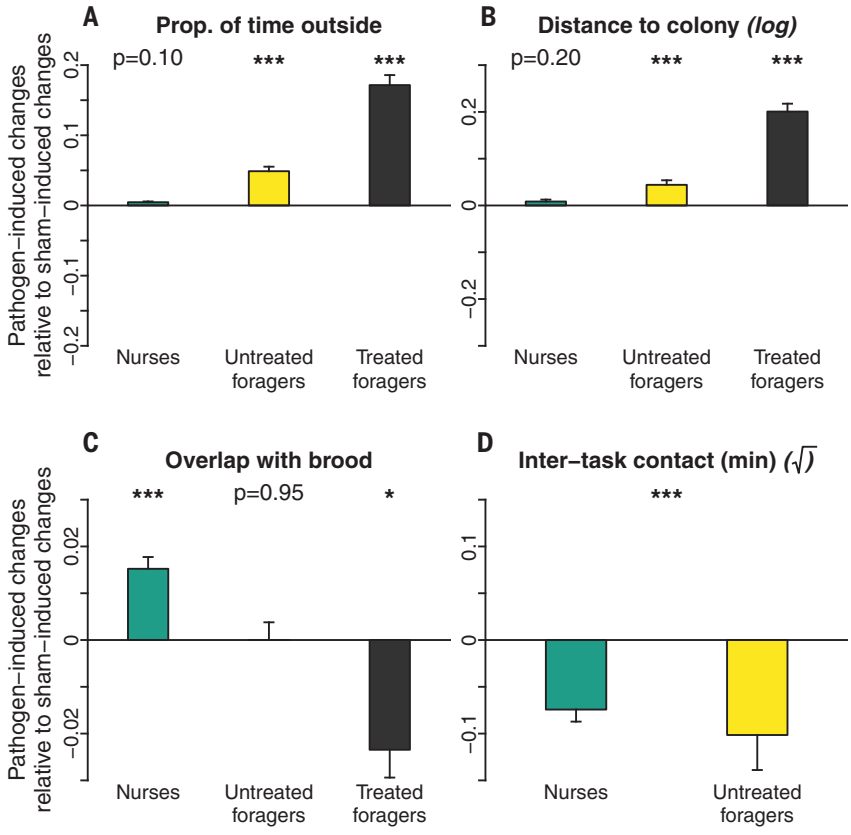

Fig. 4. Pathogen-induced changes in individual behavior. (**A** to **D**) Pathogen-induced changes in the proportion of time individual ants spent outside the nest (A), their distance to colony members (in millimeters measured between the center of gravity of the workers of interest and the rest of the colony) (B), their overlap with the brood (Bhattacharyya's affinity index) (C), and the duration of contact between untreated workers from a given task group (nurses or foragers) and untreated workers from the other task group (D). Visual representation as in Fig. 1F. Statistical analysis on all raw data. For (A) to (C), $*P < 0.05$ and $***P < 0.0001$ (GLMM, post hoc comparisons between pathogen-induced and sham-induced changes, BH corrected). For (D), $***P < 0.0001$ (GLMM, $\text{interaction}_{\text{period}\times\text{treatment}}$). Sample sizes are as in Fig. 3.

contamination loads identified in our simulations have the expected effects on individual survival, we used data from the survival experiment to compare the 9-day mortality of workers predicted to have received either a high or a low load in the simulations. As expected, workers predicted to have received a low load did not experience any detectable change in mortality, whereas workers predicted to have received a high load experienced a greater than twofold increase in mortality around 4 days after treatment (Fig. 3C). This load-dependent difference in mortality was notably observed among workers that had few direct contacts with pathogen-exposed foragers (fig. S11), underscoring the value of using a whole-network approach rather than only considering direct contacts with contaminated individuals to study disease transmission.

Further analyses revealed that the pathogen-induced changes in network properties resulted from behavioral changes not only among pathogen-exposed foragers but also among their untreated nestmates. First, pathogen-exposed foragers actively isolated themselves: They spent more time outside, increased their average distance to the rest of the colony, and reduced their area of movement while inside the nest (GLMM: $|z\ \text{score}| \geq 5.82$, $P < 0.0001$ in post hoc comparisons with BH correction; Fig. 4, A and B, fig. S14, and table S3). This led to a decrease in contact time between pathogen-exposed foragers and all untreated workers ($|z\ \text{score}| \geq 3.61$, $P \leq 0.00047$; fig. S14 and table S3). Untreated foragers also actively isolated themselves: They spent more time outside and increased their average distance to the rest of the colony ($|z\ \text{score}| \geq 3.54$, $P < 0.00061$; Fig. 4, A and B, and table S3). By contrast, nurses increased their spatial overlap with the brood ($z\ \text{score} = -4.43$, $P < 0.0001$; Fig. 4C and table S3) and moved the brood deeper inside the nest (GLMM: $\chi^2 = 22.68$, df = 1, $P < 0.0001$; fig. S14 and table S3). This led to a decrease in contact time between untreated foragers and nurses in pathogen-exposed colonies ($\chi^2 = 68.85$, df = 1, $P < 0.0001$; Fig. 4D and table S3). These pathogen-induced changes in the behavior of untreated workers contributed at least in part to the changes in overall network structure described above, as similar, lower-magnitude effects were observed in networks that excluded experimentally treated foragers (modularity and task assortativity: nonsignificant trends, $\chi^2 \leq 2.13$, df = 1, $P \geq 0.14$; clustering and efficiency: significant effects, $\chi^2 \geq 4.35$, df = 1, $P \leq 0.037$; fig. S15).

Overall, this study shows that both pathogen-exposed and untreated workers are able to rapidly detect the presence of a pathogen and immediately adjust their behavior to reinforce the disease-inhibitory effects of the colony's social network, thus reducing individual contamination risk. Such an early response, occurring before pathogen-exposed workers develop an infection, could potentially be triggered by chemical or mechanical cues associated with the fungal spores (*19*, *25*), though little is currently known about the detection mechanisms involved. Social network plasticity may represent a widespread strategy for collective resilience in the face of environmental hazards, conferring groups with an effective and easy-to-implement mechanism of response to external and internal disturbance.

REFERENCES AND NOTES

1. M. Barthélemy, A. Barrat, R. Pastor-Satorras, A. Vespignani, *J. Theor. Biol.* **235**, 275–288 (2005).
2. K. T. D. Eames, M. J. Keeling, *Proc. Natl. Acad. Sci. U.S.A.* **99**, 13330–13335 (2002).
3. R. K. Hamede, J. Bashford, H. McCallum, M. Jones, *Ecol. Lett.* **12**, 1147–1157 (2009).
4. J. O. Lloyd-Smith, S. J. Schreiber, P. E. Kopp, W. M. Getz, *Nature* **438**, 355–359 (2005).
5. D. P. Mersch, A. Crespi, L. Keller, *Science* **340**, 1090–1093 (2013).
6. T. O. Richardson, T. E. Gorochowski, *J. R. Soc. Interface* **12**, 20150705 (2015).
7. T. O. Richardson *et al.*, *PLOS Comput. Biol.* **13**, e1005527 (2017).
8. P. Sah, S. T. Leu, P. C. Cross, P. J. Hudson, S. Bansal, *Proc. Natl. Acad. Sci. U.S.A.* **114**, 4165–4170 (2017).
9. M. Salathé, J. H. Jones, *PLOS Comput. Biol.* **6**, e1000736 (2010).
10. E. M. Volz *et al.*, *PLOS Comput. Biol.* **7**, 10.1371/annotation/85b99614-44b4-4052-9195-a77d52dbdc05 (2011).
11. C. L. Nunn *et al.*, *Philos. Trans. R. Soc. London B Biol. Sci.* **370**, 20140111 (2015).
12. S. Cremer, C. D. Pull, M. A. Fürst, *Annu. Rev. Entomol.* **63**, 105–123 (2018).
13. S. Cremer *et al.*, *Curr. Biol.* **17**, R693–R702 (2007).
14. N. Stroeymeyt *et al.*, *Curr. Opin. Insect Sci.* **5**, 1–15 (2014).
15. D. Naug, S. Camazine, *J. Theor. Biol.* **215**, 427–439 (2002).
16. D. Naug, B. Smith, *Proc. Biol. Sci.* **274**, 61–65 (2007).
17. C. D. Pull, W. O. H. Hughes, M. J. F. Brown, *Naturwissenschaften* **100**, 1125–1136 (2013).
18. S. Angelone, M. J. Bidochka, *J. Invertebr. Pathol.* **156**, 73–76 (2018).
19. M. Konrad *et al.*, *PLOS Biol.* **10**, e1001300 (2012).
20. T. Brütsch *et al.*, *Ecol. Evol.* **7**, 2249–2254 (2017).
21. P. C. Lopes *et al.*, *Sci. Rep.* **6**, 31790 (2016).
22. S. Vestergaard *et al.*, *J. Invertebr. Pathol.* **73**, 25–33 (1999).
23. R. B. Rosengaus *et al.*, *Naturwissenschaften* **86**, 588–591 (1999).
24. L. Liu *et al.*, *Sci. Rep.* **5**, 15106 (2015).
25. W. O. H. Hughes *et al.*, *Proc. Biol. Sci.* **269**, 1811–1819 (2002).
26. N. Stroeymeyt *et al.*, Social network plasticity decreases disease transmission in a eusocial insect. Zenodo (2018); https://doi.org/10.5281/zenodo.1322669
27. N. Stroeymeyt *et al.*, Social network plasticity decreases disease transmission in a eusocial insect. Zenodo (2018); https://doi.org/10.5281/zenodo.1322676
28. V. Latora, M. Marchiori, *Phys. Rev. Lett.* **87**, 198701 (2001).

ACKNOWLEDGMENTS

We thank F. Bienert, A. Pagano, T. Studer, and F. Rein for their help with ant marking; U. Behrmann and D. Segalla for their help with data curation; B. Kheradmand and K. Seif for running preliminary trials that facilitated the study; S. Metzler and M. Konrad for providing dose-survival data in the *L. neglectus*–*M. brunneum* host-pathogen

system; J. Eilenberg for providing the *M. brunneum* fungal strain; and M. Chapuisat, D. Farine, R. Poulin, T. Richardson, B. Casillas-Perez, and three anonymous reviewers for commenting on previous versions of the manuscript. **Funding:** This project was funded by two European Research Council Advanced Grants (Social Life, 249375, and resiliANT, 741491) and two Swiss National Science Foundation grants (CR32I3_141063 and 310030_156732) to L.K. and a European Research Council Starting Grant (SocialVaccines, 243071) to S.C. **Author contributions:** N.S., L.K., and S.C. designed the research. A.C. and D.P.M. developed hardware and software for the production and curation of tracking data. N.S. and A.V.G. performed the research. N.S. analyzed the data and wrote the manuscript with extensive feedback from L.K. and S.C. All authors commented on the manuscript. **Competing interests:** The authors declare no competing interests. **Data and materials availability:** Data are available at (*26*) and codes are available at (*27*) and https://github.com/laurentkeller/anttrackingUNIL.

SUPPLEMENTARY MATERIALS

www.sciencemag.org/content/362/6417/941/suppl/DC1
Materials and Methods
Figs. S1 to S15
Tables S1 to S5
References (*29*–*57*)

2 March 2018; accepted 22 October 2018
10.1126/science.aat4793

Science

Social network plasticity decreases disease transmission in a eusocial insect

Nathalie Stroeymeyt, Anna V. Grasse, Alessandro Crespi, Danielle P. Mersch, Sylvia Cremer and Laurent Keller

Science **362** (6417), 941-945.
DOI: 10.1126/science.aat4793

Protecting the colony

When we get a cold and then stay home from work, we are not only taking care of ourselves but also protecting others. Such changes in behavior after infection are predicted in social animals but are difficult to quantify. Stroeymeyt *et al.* looked for such changes in the black garden ant and found that infected workers did alter their behavior—and healthy workers altered their behavior toward the sick. The changed behavior was especially valuable for protecting the most important and vulnerable members of the colony.

Science, this issue p. 941